International Journal of Mechanical, Industrial and Aerospace Sciences
ISSN: 2517-9950
Vol:2, No:5, 2008

Effects of Rarefaction and Compressibility on Fluid Flow at Slip Flow Regime by Direct Simulation of Roughness

M. Hakak Khadem, M. Shams, and S. Hossainpour

***Abstract*—**A two dimensional numerical simulation has been performed for incompressible and compressible fluid flow through microchannels in slip flow regime. The Navier-Stokes equations have been solved in conjunction with Maxwell slip conditions for modeling flow field associated with slip flow regime. The wall roughness is simulated with triangular microelements distributed on wall surfaces to study the effects of roughness on fluid flow. Various Mach and Knudsen numbers are used to investigate the effects of rarefaction as well as compressibility. It is found that rarefaction has more significant effect on flow field in microchannels with higher relative roughness. It is also found that compressibility has more significant effects on *Poiseuille number* when relative roughness increases. In addition, similar to incompressible models the increase in average fRe is more significant at low Knudsen number flows but the increase of Poiseuille number duo to relative roughness is sharper for compressible models. The numerical results have also validated with some available theoretical and experimental relations and good agreements have been seen.

***Keywords*—**Relative roughness, slip flow, Poiseuille number.

I. Introduction

IN order to design microdevices properly, it is necessary to establish the physical laws governing the fluid flow and heat transfer in microgeometry. However, it has been reported that phenomena in microgeometry may differ from those in macroscopic counterparts. Several factors that are dominant in micro scale have been identified through a number of experimental, analytical and numerical works. Among them, noncontinuum effect, compressibility effect, and various surface effects have been under vigorous investigation.

At the microscale level, it is impossible to obtain a completely smooth wall surface. According to the traditional knowledge for macrosystems, when the relative roughness is less than 5%, its effect on the friction factor is negligible. But for microscale channels, previously reported experimental and computational results have drawn a conclusion that surface roughness has a significant influence on flow and heat transfer [1, 2]. For example, the experiment by Kandlikar et al. [2] indicated that for a 0.62 mm tube with relative roughness of 0.355%, the effect of roughness on the friction factor and heat transfer was significant. Mala and Li [3] observed that for rough channels with diameters ranging from 50 to 254 lm (relative roughness height 0.7–3.5%), the pressure gradient was higher than that predicted by the classical theory and the friction factor increased when the Re number was increased. In addition, an early transition from laminar to turbulent flow occurred at the Reynolds number less than 2300. They concluded that these phenomena can be well explained due to the surface roughness effects.

In some experimental works such as Wu and Little [4, 5], friction factors have been measured for both laminar and turbulent flows in miniaturized channels etched in silicon and glass. The hydraulic diameter of trapezoidal-cross-section microchannels ranged from 45.46 to 83.08 mm. The measured values of the friction factor were much larger (e.g., 10–30% in silicon channels and 3–5 times in glass channels) than those predicted by the conventional correlation for a smooth circular tube. They attributed their anomalous results to the large relative (and asymmetric) roughness of test channels (actually, the equivalent relative roughness was estimated to be in the range of 0.2 to 0.3 through indirect measurement). Choi et al. [6] measured friction factors of nitrogen flow in microtubes of diameter ranging from 3 to 81 mm. The measured friction factors for laminar and turbulent flows were found to be consistently smaller than those predicted by the macro scale correlation in macro tubes. For laminar flow ($Re < 2{,}300$), the friction constant, C, was 19–27% smaller than the conventional one, with an average friction constant of 53, instead of 64.

In modeling of roughness effect on rarefied flows, Usami et al. [7] studied rarefied gas flow through a 2D channel using a DSMC method by varying the surface roughness distribution and the Kn number. The reduction of flow conductivity caused by surface roughness was obtained in the transition regime. Sun's study [8] by using a DSMC method found that the roughness element size had a significant effect on the friction factor of rarefied flows when $0.01 < Kn < 0.1$. Karniadakis et al. [9] applied a more accurate gas flow model and found that the roughness effect becomes more significant on rarefied flows when the Kn number was increased.

M. Hakak Khadem is with the Mechanical Engineering Department, Sahand University of Technology, Tabriz, Iran (e-mail: masoudhak2007@yahoo.com).

M. Shams is with the Mechanical Engineering Department, K. N. Toosi University of Technology, Tehran, Iran (e-mail: shams@kntu.ac.ir).

S. Hossainpour is with the Mechanical Engineering Department, Sahand University of Technology, Tabriz, Iran (phone: +98-412-3459053; fax: +98-412-3444300; e-mail: hossainpour@sut.ac.ir, corresponding author).

However, for a rarefied gas flowing in a microchannel, the roughness effect is more complex and difficult to measure [10]. Experimental investigation by Sugiyama [11,12] demonstrated that the conductance of an unsteady rarified flow between two flat, rough plates decreased significantly with decrease in Kn when Kn > 1. It reached the minimum value around Kn = 0.5, and with further decrease in Kn, the conductance increased rapidly. Their calculation also showed that a pronounced effect of the wave angle on the flow conductance, when Kn = 1 and Kn = 0.1. They did not investigate the roughness effect on rarefied flow in the slip regime (0.001 < Kn < 0.1).

There are also some studies on direct simulation of roughness. Valdes et al [13] have numerically investigated the roughness effect on laminar incompressible flow through microchannels. In their work the roughness is simulated by the superimposition of randomly generated triangular peaks on the inner wall of a smooth microchannel. In recent research Ji et al. [14] studied the influence of roughness in slip flow regime with second order slip boundary conditions. They simulated the roughness with rectangular elements on two parallel plates with different spacing and heights to investigate the effect of wall roughness on friction factor and Nusselt number. They showed that the effect of wall roughness is reduces with increasing Knudsen number.

In this study we will focus on slip flow regime (0.001 < Kn < 0.1) that requires the use of slip boundary conditions. Although there are several models for slip boundary conditions, we will use Maxwell model for slip and Smoluchowskyi for temperature jump conditions that will be discussed later. Compressibility and rarefaction effect on fluid flow will be taken into consideration.

II. Problem Definition and CFD Model

A. Model Development

We consider a pressure-driven gas flow between two long parallel plates. Fig. 1 shows a schematic of the *2D* flow through a rough channel with length *L* and height *H*. to simulate roughness on channel surfaces we considered triangular peaks with height *r* and width *w* for all of the models. These elements are uniformly and symmetrically distributed on the top and bottom surfaces. Although, this geometry is not exactly the same as the actual rough surface, it is considered as a close approximation to investigate the roughness effect on the flow field and pressure distribution. This was also studied in a work by Ji et al but they assumed roughness as rectangular microelements. The distance between the two plates is considered as *H*, which is also the characteristic length of the flow system. For the rough elements, the peak to peak spacing is shown with *s*. A parameter called *''relative roughness height''* is defined as *e = r/H*. In most microfluidic systems, the relative roughness heights are estimated at 0.1–6%. We adopt this roughness height range for the study. From the above discussion, we know that the rarefaction effect cannot be neglected. In addition, for the pressure driven gas flow, when the channel length is much larger than the channel height *(L >> H)*, even in the low Reynolds number range, the Mach number can reach a higher value due to small hydraulic diameter and higher pressure drop.

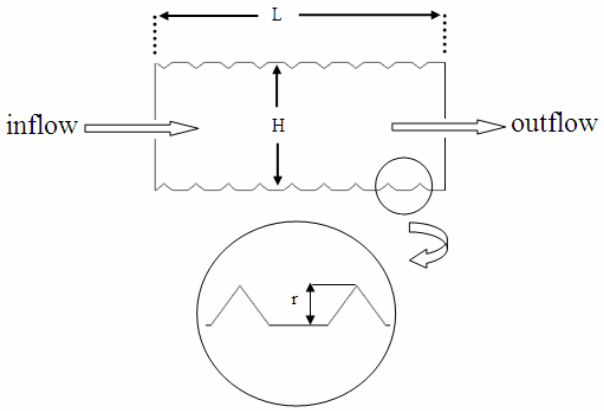

Fig. 1 Microchannel with roughed walls and a closed view of roughness elements

B. Governing Equations

In slip flow regime, for steady laminar flow of compressible fluid with constant thermophysical properties, the governing equations are continuity, momentum, energy and the gas state equations that must be solved with appropriate boundary conditions which will be stated in the next section. These equations have been shown bellow.

$$\frac{\partial(\rho u)}{\partial x}+\frac{(\rho v)}{\partial y}=0 \tag{1}$$

$$\rho u\frac{\partial u}{\partial x}+\rho v\frac{\partial u}{\partial y}=-\frac{\partial P}{\partial x}+\mu\left[\frac{\partial^2 u}{\partial x^2}+\frac{\partial^2 u}{\partial y^2}+\frac{1}{3}(\frac{\partial^2 u}{\partial x^2}+\frac{\partial^2 v}{\partial x\partial y}\right] \tag{2}$$

$$\rho u\frac{\partial v}{\partial x}+\rho v\frac{\partial v}{\partial y}=-\frac{\partial P}{\partial y}+\mu\left[\frac{\partial^2 v}{\partial x^2}+\frac{\partial^2 v}{\partial y^2}+\frac{1}{3}(\frac{\partial^2 v}{\partial x^2}+\frac{\partial^2 u}{\partial x\partial y}\right] \tag{3}$$

$$\rho c_p u\frac{\partial T}{\partial x}+\rho c_p v\frac{\partial T}{\partial y}= \frac{\partial}{\partial x}(K\frac{\partial T}{\partial x})+\frac{\partial}{\partial y}(K\frac{\partial T}{\partial y})+u\frac{\partial P}{\partial x}+v\frac{\partial P}{\partial y} +\mu\left[2(\frac{\partial u}{\partial x})^2+2(\frac{\partial v}{\partial y})^2+(\frac{\partial u}{\partial y}+\frac{\partial v}{\partial x})^2\right]-\frac{2}{3}\mu(\frac{\partial u}{\partial x}+\frac{\partial v}{\partial y})^2 \tag{4}$$

$$P=\rho RT \tag{5}$$

Where T, ρ_i, P, u and v are the gas temperature, density, pressure, streamwise velocity, and normal velocity, respectively. C_p, μ and K are the specific heat, viscosity and thermal conductivity of the gas, which are taken as constant. The above equations are non dimensionalized with respect to the channel height *H*, inlet mean velocity u_i, inlet temperature T_i, inlet mean density ρ_i and inlet pressure P_i. Also some of important dimensionless numbers that have been used are shown bellow:

$$\eta\frac{\partial(\rho^*U)}{\partial X}+\frac{\partial(\rho^*V)}{\partial Y}=0 \quad (6)$$

$$\mathrm{Re}_i\ \rho^*(\eta U\frac{\partial U}{\partial X}+V\frac{\partial V}{\partial Y})= \quad (7)$$
$$-\frac{\eta\,\mathrm{Re}_i}{\gamma {Ma_i}^2}\frac{\partial P^*}{\partial X}+[\eta^2\frac{\partial^2U}{\partial X^2}+\frac{\partial^2U}{\partial Y^2}+\frac{1}{3}(\eta^2\frac{\partial^2U}{\partial X^2}+\eta\frac{\partial^2V}{\partial X\partial Y})]$$

$$\mathrm{Re}_i\ \rho^*(\eta U\frac{\partial V}{\partial X}+V\frac{\partial V}{\partial Y})= \quad (8)$$
$$-\frac{\eta\,\mathrm{Re}_i}{\gamma {Ma_i}^2}\frac{\partial P^*}{\partial Y}+[\eta^2\frac{\partial^2V}{\partial X^2}+\frac{\partial^2V}{\partial Y^2}+\frac{1}{3}(\eta^2\frac{\partial^2V}{\partial X^2}+\eta\frac{\partial^2U}{\partial X\partial Y})]$$

$$\eta U\frac{\partial\theta}{\partial X}+V\frac{\partial\theta}{\partial Y}= \quad (9)$$
$$\frac{1}{Pe_i\rho^*}[\eta^2\frac{\partial}{\partial X}(\frac{\partial\theta}{\partial X})+\frac{\partial}{\partial Y}(\frac{\partial\theta}{\partial Y})+Ec_i\frac{P_i}{\rho_i{u_i}^2\rho^*}[\eta U\frac{\partial P}{\partial X}+V\frac{\partial P}{\partial Y}]$$
$$+\frac{Ec_i}{\mathrm{Re}_i\rho^*}[2(\frac{\partial U}{\partial X}\eta)^2+2(\frac{\partial V}{\partial Y})^2+(\frac{\partial V}{\partial X}\eta+\frac{\partial U}{\partial Y})^2-\frac{2}{3}(\frac{\partial U}{\partial X}\eta+\frac{\partial V}{\partial Y})^2]$$

Where the parameters for non-dimensionalizing are:

$$\theta=\frac{T-T_w}{T_i-T_w},\ \eta=\frac{H}{L},\ X=\frac{x}{L},\ Y=\frac{y}{H},\ \rho^*=\frac{\rho}{\rho_i}$$
$$P^*=\frac{P}{P_i},\ U=\frac{u}{u_i},\ V=\frac{v}{u_i},\ C_p=\frac{C_p}{C_{pi}},\ K^*=\frac{K}{K_i}$$

And important dimensionless parameters are:

$$\mathrm{Re}_i=\frac{\rho_i u_i H}{\mu},\ Ma_i=\frac{u_i}{\sqrt{\gamma RT_i}},\ Pe_i=\frac{u_i H}{\alpha_i},\ Kn_i=\sqrt{\frac{\pi\gamma}{2}}\frac{Ma_i}{\mathrm{Re}_i}$$

C. Boundary Conditions

As we know, in slip flow regime that is specified with Knudsen number between 0.001 and 0.1, we have to use slip boundary conditions with Navier-Stokes equations "1-4". To do so, there are some models that recently have been validated and used by various authors such as, second order slip model [1], Langmuir [15], and some other first and second order boundary conditions. But here we will use the most general one that are Maxwell and von Smoluchowski's for slip and temperature-jump boundary conditions given by [16]. These boundary conditions are shown bellow in Cartesian form:

$$u_{fluid}-u_{wall}=\frac{2-\sigma_v}{\sigma_v}\lambda\frac{\partial u}{\partial y}+\frac{3}{4}\frac{\mu}{\rho T}\frac{\partial T}{\partial x}, \quad (10)$$

$$T_{fluid}-T_{wall}=\frac{2-\sigma_v}{\sigma_v}\frac{2\gamma}{\gamma+1}\frac{\lambda}{\mathrm{Pr}}\frac{\partial T}{\partial y} \quad (11)$$

Where we have used following definitions for Knudsen number and mean free path respectively:

$$Kn=\frac{\lambda}{L} \quad (12)$$

$$\lambda=\frac{kT}{\sqrt{2}\pi\sigma^2P} \quad (13)$$

These formulations apply to flat surfaces in non-rotating domains. As it was noted by other investigators, neglecting the influence of surface curvature or rotating motion on slip behavior leads to false prediction. Introducing necessary modifications for those cases extended, formulations have been proposed:

$$u_{fluid}-u_{wall}=\frac{2-\sigma_v}{\sigma_v}\lambda(\frac{\partial u}{\partial n}+\frac{\partial u}{\partial t})+\frac{3}{4}\frac{\mu}{\rho T}\frac{\partial T}{\partial t}, \quad (14)$$

Where *n* and *t* are stand for normal and tangential to surface at each point of the wall.

Choosing full accommodation ($\sigma_v=1$), there are several good agreements with experimental data in various works but they were all chosen for smooth surfaces. For nitrogen, that is our working fluid too, Table I shows values proposed by some authors.

TABLE I
FITTING PARAMETERS OBTAINED FROM SOME EXPERIMENTAL WORKS

Previous studies	Accommodation coefficient
Porodnov(1974) [17]	0.925± 0.014
Arkilic(1997) [18]	0.81±0.96
Maurer(2003) [19]	0.87± 0.03
Colin(2004) [20]	0.93
Ewart(2007) [21]	0.908±0.041

In this paper we chose $\sigma_v=0.9$ as was chosen by Ji et al [1] in their study for rectangular roughness elements and is acceptable with respect to Table I.

The other boundary conditions are at inlet and outlet of the channel illustrated bellow:

At X=0 $\quad P^*=1, V=0, \theta=1$

At X=1 $\quad P^*=P_{out}/P_i$

To reduce the computation work only one half of the channel is considered due to the symmetrical conditions that are applied at *Y=0.*

D. CFD Model and Numerical Solution Details

As we know the rarefaction and compressibility effects play important roles in gaseous flows and lead to different flow characteristics. These effects are closely related to the microchannel dimensions, inlet Mach number, and the roughness elements, etc. So we have chosen low and high inlet Mach and Knudsen numbers to highlight these effects. Our simulation is based on six models that are shown in table 2. For models 1 and 2 we have chosen two Mach numbers to highlight the effects of compressibility. Other models are to show the effects of both rarefaction and compressibility. All models have aspect ratio of 5 (L/H=5), and the peak density of 10, that is the number of triangular roughness elements in 0.1mm.

Air is chosen as the working gas. The inlet flow total temperature is 300 K. The wall temperature is set at 320 K.

A finite volume based CFD code was used to solve flow equations with associating boundary conditions (equations 10 and 11). Also SIMPLE algorithm has been used in body fitted

coordinate system to descritize governing equations. The entire microchannel length is taken as the computational domain to investigate the effect of roughness on the flow field. Because of triangular shapes of the roughness elements we have selected triangular mesh all over the computational domain. The grids are refined near the wall region to obtain highly accurate numerical solutions around the roughness elements. For example the grids that are used in models 5 have shown in Fig. 2. To evaluate the grid size effect on the accuracy of numerical solutions, grid-independence tests were performed as the grid size was refined until acceptable differences between the last two grid sizes were found. For example, we have used the following four grid sizes: 480×64, 280×48, 160×32 and 128×24. For model 1 with Kn=0.0033, Ma=0.1 and e = 0.75%, The maximal difference in fRe were 0.73%, 1.85%, 4% respectively. By balancing between the computation time and accuracy, the grid size 280×48 was selected.

TABLE II
DETAILS OF SIX MODELS USED IN THIS STUDY

Models	Kn	Ma	Relative roughness (%)
Model 1	0.003	0.005, 0.02	5, 3.75, 2.5, 1.25, smooth
Model 2	0.003	0.25, 0.4	5, 3.75, 2.5, 1.25, smooth
Model 3	0.01	0.005	5, 3.75, 2.5, 1.25, smooth
Model 4	0.01	0.25	5, 3.75, 2.5, 1.25, smooth
Model 5	0.033	0.005	5, 3.75, 2.5, 1.25, smooth
Model 6	0.033	0.25	5, 3.75, 2.5, 1.25, smooth

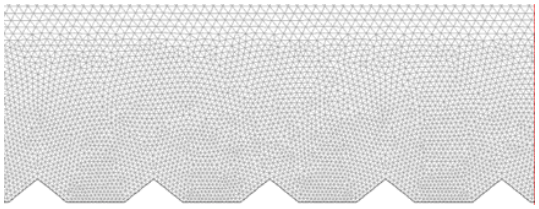

Fig. 2 The near wall grid for computational domain of model 5

III. RESULTS AND DISCUSSION

In this section the effects of wall roughness on rarefied, compressible and incompressible flow are investigated for two cases that have been generated and discussed before. Although there are many parameters related with surface roughness, here we focused on *Poiseuille* number witch is the most important parameter in analyzing roughness effects. Then we will compare results and discuss the differences between related models.

A. Poiseuille Number, Slip Velocity and Pressure Gradient

As we know, *Poiseuille* number is a factor for friction measurements and is defined as the product of friction factor and local Reynolds number ($Po = f.\mathrm{Re}$) and we will later use equation 15 to compute it for each model.

$$f.\mathrm{Re} = \frac{-2(d\bar{P}/dx).D_h}{\mu\bar{u}} \qquad (15)$$

Where, D_h, is hydraulic diameter that is *2H* for the case of two parallel plates, and $d\bar{P}/dx$ is the average pressure gradient in the flow direction. It must be noted that since pressure is decreasing through flow direction, the Knudsen number increases along a microchannel in *Poiseuille* flow. Consequently, axial velocity varies with axial distance, lateral velocity component does not vanish, streamlines are not parallel, and pressure gradient is not constant. For this case of study (tow parallel plates), the acceptable value for *Poiseuille* number in conventional channels is *Po*=96 and is independent of surface roughness. But in microchannels Beskok and Karniadakis [22] recommended a simple equation fRe = 96/ (1 + 6Kn) to evaluate the *Poiseuille* number for the incompressible rarefied flow, with a first order boundary condition and an accommodation coefficient of unity. Later we will show good agreement of this equation with numerical results of our study.

Fig. 2 shows velocity distribution on centerline and slip velocity on the rough wall of model 7 with Mach number of 0.02 and relative roughness of 5%.

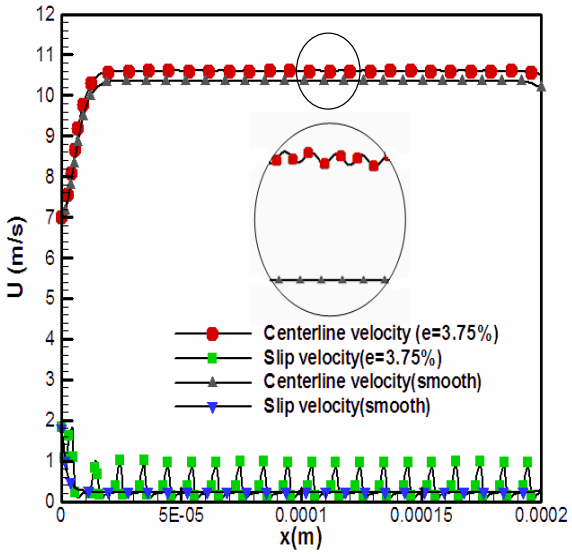

Fig. 3 Centerline and slip velocity for rough and smooth cases of model 1 (Mach=0.02)

It can be seen that roughness peaks are associated with higher slip velocity and also results in higher centerline velocity compare to that of smooth channel. In addition it is found that the mass flow rate for this model will be almost 15% less than that of smooth channel because of obstruction effect. The gas is compressed in the narrower space and expanded in the wider space, which results in the velocity field experiencing a periodical expansion– compression cycle.

B. Rarefaction Effect

In this section, we focus on the effects of roughness in conjunction with rarefaction condition on the gas flow.

Models 1, 3 and 5 are designed to address these two effects together. Fig. 4 shows the local friction factor for the smooth channels with different inlet Kn numbers. It is clear that fRe is significantly lower for the flow with a higher Kn than that with a lower Kn number. However, near the entrance, the values of fRe decrease sharply. Then, the downstream values of fRe decrease slightly along the flow direction. This small change in the *Poiseuille* number along the channel results from an insignificant increase of the Kn number. As discussed above, Beskok and Karniadakis recommended a simple equation fRe = 96/ (1 + 6Kn) to evaluate the *Poiseuille* number for the rarefied flow with a first order boundary condition and an accommodation coefficient of unity. Comparing results from Beskok and Karniadakis with our results indicates a similar trend except near the entrance region, where our results show an entrance effect. In general, our results are slightly lower. This comes mainly from the lower momentum and energy accommodation coefficients. The lower *Poiseuille* number is expected, since the slip condition implies less shear stress against the wall and a higher Kn means larger slip. Therefore, the flow near the entrance is sensitive to the geometry and fRe results in high values, while downstream from the entrance, the fRe shows smaller decreases.

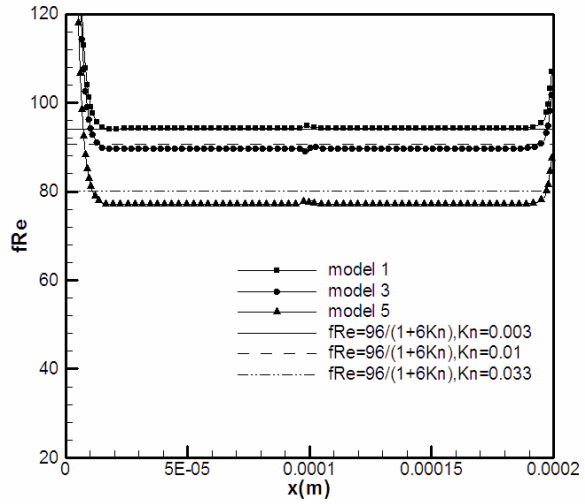

Fig. 4 Effect of Knudsen number on f.Re along smooth channels (numerical and analytical results).

The average fRe for a rough channel is plotted against the relative roughness height in Fig. 5. The average fRe is evaluated based on the non-entrance region. For the flow with a lower inlet Kn number (Model 1), the average fRe increase by 2%, 4.5%, 7.1%, and 11% compared with a smooth channel for relative roughness heights of 1.25%, 2.5%, 3.75% and 5%, respectively while for high Knudsen flow of Model 5 these values are : 1.9%, 4%, 8.1%, 14.3% respectively. It seems that roughness has more effect on higher Knudsen number flows with higher relative roughness. This is because the increase in collision rate between rough wall and gas molecules in higher Knudsen number flows.

However for the gas with a lower Kn number and relative roughness the stagnation region between roughness elements causes a greater pressure drop and a higher increase in fRe. Similar results can also be found in the study of Ji [1]. Their calculations indicated that when the Kn number increased from 0.0044 to 0.033, fRe significantly decreased.

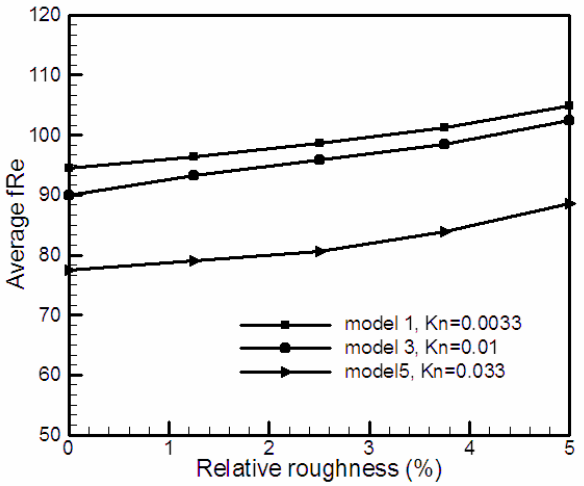

Fig. 5 Average fRe against relative roughness with different Kn numbers for incompressible models.

C. Compressibility Effect

In the transport of a gas by microchannels, great changes in properties of the gas occur because of large pressure drop caused by the friction effects even when the flow velocity is small. For example, pressure drops of several atmospheres were observed in a 4 mm long channel [23] due to the viscous friction. Friction contributes to large pressure gradient, which in turn generates changes in gas density. In order to satisfy mass conservation, the gas must accelerate as its density decreases with the decreasing pressure towards the exit of the channel. Acceleration effect on the total pressure drop caused by the change of density must be considered. In this section, we will examine the effect of wall roughness together with the gas compressibility. Models 2, 4 and 6 were designed to highlight the compressibility importance.

There are several analytical and experimental equations that predict *Poiseuille* number for compressible flows. Equations 16, 17 are the two that were also used by Tang [24].

$$\frac{(f\,\mathrm{Re})_{co}}{(f\,\mathrm{Re})_{inc}} = (1 - 0.143Ma + 1.273Ma^2) \tag{16}$$

$$\frac{(f\,\mathrm{Re})_{co}}{(f\,\mathrm{Re})_{inc}} = (1 + \frac{Ma^2}{1.5 - 0.66Ma - 1.44Ma^2}) \tag{17}$$

Comparing our result with these equations, of course for models with low Kundsen number, shows good agreements. For example for Model 2 with average Mach number of 0.25, by use of equations 16 and 17, fRe will be 100.2 and 100.8 respectively while our simulation results in 99. Ignoring the rarefaction effects in equations 16 and 17, results in lower value this parameter. But there is no correlation for rarefied,

compressible flows and we just know that rarefaction will reduce the friction coefficient.

Fig. 6 shows the increase of average fRe for smooth and rough channels duo to increase in Mach number. For the incompressible flow, the *Poiseuille* number stays constant with a very large Reynolds number for a given relative roughness height. However, for a compressible flow, the average fRe shows significant increases. Also it demonstrates the effect of relative roughness on *Poiseuille* number at high Mach numbers. As the relative roughness increases the increase in Poiseuille number becomes more significant. Since the Mach number is a compressibility scale, the existence of larger roughness can cause larger pressure drop and result in larger Poiseuille number.

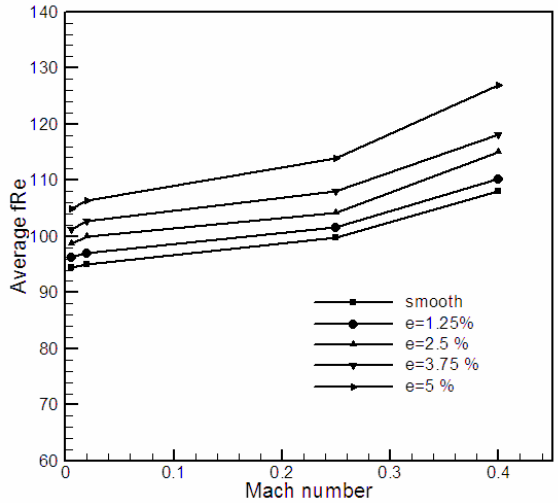

Fig. 6 Average fRe for smooth and rough channels with different Mach numbers

This result can be seen in the study of Turner et al. [25] too. They demonstrated that when relative surface roughness was small, there was no clear effect on the friction factor for rarefied and compressible flows. The increase in fRe appeared to be quite small and is within 2–6%.

The increase of *Poiseuille* number for three compressible models is plotted against surface relative roughness, for various Knudsen numbers in Fig. 7. Similar to incompressible models the increase in average fRe is more significant at low Knudsen number flows but the increase of *Poiseuille* number duo to relative roughness is sharper for compressible models. This is because of higher pressure drop associated with collisions between rough surface and gas molecules happening in channels with higher Mach number. Fig. 8 show this effect by comparing the contours of pressure gradient for compressible and incompressible models 1(Mach=0.02) and 2(Mach=0.25). A great pressure drop can be seen on top of the roughness elements that is the major reason of increasing average fRe. We can also see more effects of roughness on entire flow filed for compressible flow witch is duo to more sensitivity of compressible flow to pressure gradient.

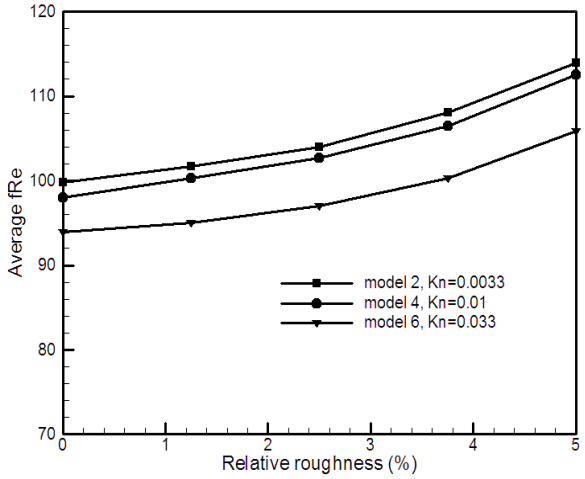

Fig. 7 Average fRe against relative roughness with different Kn numbers

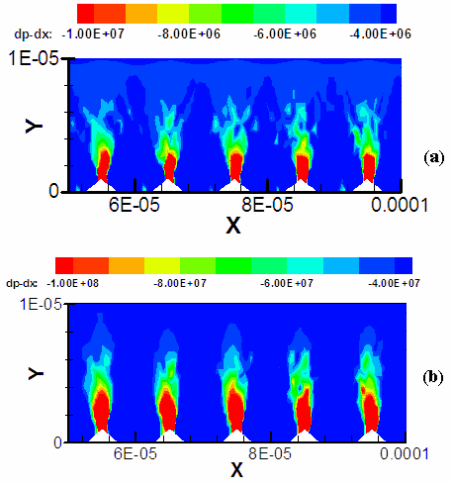

Fig. 8 Contours of pressure gradients for (a) incompressible flow of model 1 with Ma=0.02 and (b) compressible flow of model 2 with Ma=0.25 (both with *e=5%*)

IV. Conclusion

The effects of wall roughness on the rarefied and compressible gas flows were evaluated and the following conclusions were reached:

(1) The rough elements restrict the upstream gas flow and cause more pressure drop and increases in the *Poiseuille* number due to the obstruction effect.

(2) The results have checked with previous analytical and experimental studies for both incompressible and compressible flows and good agreements were achieved.

(3) The compressible flow is more sensitive to relative roughness duo to higher pressure gradients and its effects on flow field.

REFERENCES

[1] Yan Ji, Kun Yuan, J.N. Chung, Numerical simulation of wall roughness on gaseous flow and heat transfer in a microchannel, Int. J. Heat Mass Transfer 49, 2006 1329–1339.
[2] S.G. Kandlikar, S. Joshi, S. Tian, Effect of channel roughness on heat transfer and fluid flow characteristics at low Reynolds numbers in small diameter tubes, in: Proceedings of NHTC_01 35th National Heat Transfer Conference, Anaheim, CA, June 2001, pp. 1–10.
[3] G.M. Mala, D. Li, Flow characteristics of water in microtubes, Int. J. Heat Mass Transfer 20 (1999) 142–148.
[4] P.Y. Wu, W.A. Little, Measurement of friction factor for the flow of gases in very fine channels used for microminiature Joule–Thomson refrigerator, Cryogenics 23 (1983) 273–277.
[5] P.Y. Wu, W.A. Little, Measurement of the heat transfer characteristics of gas flow in fine channel heat exchangers used for microminiature refrigerators, Cryogenics 24 (1984) 415–420.
[6] S. B. Choi, R. F. Barron, and R. O. Warrington, Fluid Flow and Heat Transfer in Microtubes,
[7] M. Usami, T. Fujimoto, S. Kato, Mass-flow reduction of rarefied flow roughness of a slit surface, Trans. Jpn. Soc. Mech. Eng., B 54 (1988) 1042–1050.
[8] H. Sun, M. Faghri, Effect of surface roughness on nitrogen flow in a icrochannel using the direct simulation Monte Carlo method, umer. Heat Transfer Part A 43 (2003) 1–8.
[9] G.E. Karniadakis, A. Beskok, Micro Flows, Fundamental and imulation, Springer, Berlin, 2002.
[10] E. Turner, H. Sun, M. Faghri, O.J. Gregory, Effect of surface roughness on gaseous flow through micro channels, 2000 IMECE, TD 366 (2) (2000) 291–298.
[11] W. Sugiyama, T. Sawada, K. Nakamori, Rarefied gas flow between two flat plates with two dimensional surface roughness, Vacuum 47 1996) 791–794.
[12] Sugiyama, T. Sawada, M. Yabuki, Y. Chiba, Effects of surface roughness on gas flow conductance in channels estimated by conical roughness model, Appl. Surf. Sci. 169–170 (2001) 787–791.
[13] R. Valses, J. Miana, Luis Pelegay, Luis Nunez, Thomas Putz. Numerical investigation of the influence of roughness on the laminar incompressible fluid flow through annular microchannels, Int. J. Heat Mass Transfer 50 (2007) 1865–1878.
[14] Yan Ji, Kun Yuan, J.N. Chung, Numerical simulation of wall roughness on gaseous flow and heat transfer in a microchannel, Int. J. Heat Mass Transfer 49 (2006) 1329–1339.
[15] Choi, Hyung-il, Lee, Dong-ho and Lee, Dohyung , (2005) 'Complex Microscale Flow Simulations Using Langmuir Slip Condition', Numerical Heat Transfer, Part A: Applications, 48:5, 407 - 425
[16] A. Beskok, G.E. Karniadakis, A model for flows in channels, pipes and ducts at micro and nanoscales, Microscale Thermophys. Eng. 3 (1999) 43–77.
[17] Porodnov BT, Suetin PE, Borisov SF, Akinshin VD (1974) J Fluid Mech 64:417–437
[18] Arkilic EB, Schmidt MA, Breuer KS (1997) J Microelectromech Syst 6(2):167–178
[19] Maurer J, Tabeling P, Joseph P, Willaime H (2003) Phys Fluid 15:2613–2621
[20] Colin S, Lalonde P, Caen R (2004) Heat Transfer Eng 25(3):23–30
[21] T. Ewart, P.Perrier, I.Graur, J.Gilbert, “Tangential momemtum accommodation in microtube”, Microfluid nanofluid, (2007) 3:689–695
[22] A. Beskok, G.E. Karniadakis, A model for flows in channels, pipes and ducts at micro and nanoscales, Microscale Thermophys. Eng. 3 (1999) 43–77.
[23] J.C. Shih, C.M. Ho, J.Q. Liu, Y.C. Tai, Monatomic and polyatomic gas flow through uniform microchannels, Microelectromechanical Syst. 59 (1996) 197–203.
[24] Z.Y. Guo, Z.X. Li, Size effect on microscale single-phase flow and heat transfer, Int. J. Heat Mass Transfer 46 (2003) 149–159.
[25] S.E. Turner, Experimental investigation of gas flow in microchannels, ASME J. Heat Transfer 126 (2004) 753–762.